Influence of Size, Surface, Cell Line, and Kinetic Properties on the Specific Binding of A33 Antigen-Targeted Multilayered Particles and Capsules to Colorectal Cancer Cells

Christina Cortez,[†] Eva Tomaskovic-Crook,[‡] Angus P. R. Johnston,[†] Andrew M. Scott,[§] Edouard C. Nice,[‡] Joan K. Heath,[‡] and Frank Caruso[†,*]

[†]Centre for Nanoscience and Nanotechnology, Department of Chemical and Biomolecular Engineering, The University of Melbourne, Victoria 3010, Australia, [‡]Ludwig Institute for Cancer Research, Melbourne Branch of Tumour Biology, Royal Melbourne Hospital, Victoria 3050, Australia, and [§]Ludwig Institute for Cancer Research, Melbourne Centre for Clinical Sciences, Austin Hospital, Heidelberg, Victoria 3084, Australia

ABSTRACT There has been increased interest in the use of polymer capsules formed by the layer-by-layer (LbL) technique as therapeutic carriers to cancer cells due to their versatility and ease of surface modification. We have investigated the influence of size, surface properties, cell line, and kinetic parameters such as dosage (particle concentration) and incubation time on the specific binding of humanized A33 monoclonal antibody (huA33 mAb)-coated LbL particles and capsules to colorectal cancer cells. HuA33 mAb binds to the A33 antigen present on almost all colorectal cancer cells and has demonstrated great promise in clinical trials as an immunotherapeutic agent for cancer therapy. Flow cytometry experiments showed the cell binding specificity of huA33 mAb-coated particles to be size-dependent, with the optimal size for enhanced selectivity at ~500 nm. The specific binding was improved by increasing the dosage of particles incubated with the cells. The level of specific *versus* nonspecific binding was compared for particles terminated with various polyelectrolytes to examine the surface dependency of antibody attachment and subsequent cell binding ability. The specific binding of huA33 mAb-coated particles is also reported for two colorectal cancer cell lines, with an enhanced binding ratio between 4 and 10 obtained for the huA33 mAb-functionalized particles. This investigation aims to improve the level of specific targeting of LbL particles, which is important in targeted drug and gene delivery applications.

KEYWORDS: antibodies · colloids · capsules · polyelectrolytes · cell targeting

Polymer capsules formed by the layer-by-layer (LbL) technique are promising carriers for the delivery of therapeutics.[1–3] These capsules are typically formed by the sequential deposition of interacting polymers on a spherical core or template (forming a core–shell particle) and subsequent dissolution of the core.[4,5] The versatility of this technique allows for the production of capsules of a predetermined size by simply varying the size of the template, as well as the preparation of capsules composed of various polymers, which may interact electrostatically, through hydrogen bonding, or by other chemistries, including disulfide linkages[6] and click chemistry.[7] The loading of such capsules with various materials such as proteins,[8–10] drugs,[11] and nucleic acid[12] has been reported. The surface of the particles can also be manipulated by applying various coatings such as poly(ethylene glycol) (PEG) to render the particles nonfouling[13,14] or by biofunctionalization for targeted delivery applications.[15,16] Recently, we reported the biofunctionalization of LbL core–shell particles and capsules with the humanized A33 monoclonal antibody (huA33 mAb), which binds specifically to A33 antigen-expressing colorectal cancer cells.[16] A 4-fold increase in binding was achieved with huA33 mAb-coated particles compared with nonfunctionalized particles. Specific binding of particles to target cells would potentially allow a high concentration of therapeutic to be delivered in targeted areas of the body.[17] By preferentially killing the desired cells and limiting the potentially harmful side effects of the drug in healthy cells, targeted delivery is expected to increase the therapeutic index of the drug.[17]

Particle binding to cells can occur either specifically, by attaching to specific moieties or receptors on the cell surface, or nonspecifically, by general interaction with one or more components of the cellular membrane. In both cases, binding is expected to be governed by the nature of the particle, including its size, composition, and surface properties. Size is an important parameter, as it ultimately dictates the

*Address correspondence to fcaruso@unimelb.edu.au.

Received for review June 6, 2007 and accepted July 27, 2007.

Published online August 14, 2007.
10.1021/nn700060m CCC: $37.00

© 2007 American Chemical Society

method of internalization of the particle as well as its ability to permeate through tissues and be targeted to the required area.[18–20] Studies have reported cellular internalization of various sized particles from several nanometers to 3 μm.[21–23] The type of cell also adds a level of complexity, as particle binding and uptake can vary depending on cell type, cell line, and cell surface properties, including surface charge, which is integral to their interaction with particles.[24,25] In general, the outer surface of cells has a net negative charge due to ionized groups on macromolecules exposed to the extracellular environment.[26] Cells can also have both positive and negative domains on the surface, as reported for pharyngeal epithelial cells.[27] The net surface charge of the particle, as well as its hydrophobicity, will therefore have an influence on particle binding to cells.[18–20,28] In addition to particle size and cell type, particle internalization is also known to depend on particle composition and surface chemistry.[18–20,28,29]

Almost all (95%) primary human colorectal tumors express the A33 antigen on the cell surface.[30,31] HuA33 mAb binds to the A33 antigen and, upon so, activates a cellular internalization mechanism that may be used for the internalization of therapeutic-loaded particles.[32] In recent years, radiolabeled huA33 mAb has been used in several clinical trials conducted in patients with colorectal cancer, with promising results.[33–35] The combination of the drug-loading ability of polymer capsules and the clinical significance of huA33 mAb as the binding ligand provides new opportunities for delivering therapeutics to colorectal tumor cells. In our recent study, we reported the selective and antigen-mediated binding of huA33 mAb-coated particles to LIM1215, a colorectal cancer-derived cell line expressing the A33 antigen.[16] In this work, the effects of various parameters such as core–shell particles *vs* capsules, dosage (particle concentration), and surface composition on the binding of huA33 mAb-coated particles to LIM1215 cells are examined. The binding of huA33 mAb-coated particles to another A33 antigen-expressing, colorectal cancer-derived cell line is also reported. Studying the effect of these parameters on the interaction of the huA33 mAb-coated particles with cells provides valuable information on the conditions for the efficient binding, and hence targeting, of huA33 mAb-functionalized particles to colorectal cancer cells. This study complements previous work on the use of LbL-engineered materials for bioapplications, where biofunctionalized LbL films on planar substrates have been used for biosensing,[36] DNA transfection,[37] and tissue engineering.[38–40]

RESULTS AND DISCUSSION

Effect of Size. To determine the optimal particle size for cellular binding, poly(sodium-4-styrenesulfonate) (PSS)-terminated core–shell particles of diameter approximately 300 nm, 500 nm, and 1 μm were biofunctionalized with huA33 mAb, and their binding to LIM1215 cells was investigated using flow cytometry. The huA33 mAb-coated particles have an antibody surface coverage of approximately 10 mg per square meter of PSS surface.[16] The binding of 500 nm and 1 μm huA33 mAb-coated core–shell particles to LIM1215 cells is shown in Figure 1. Figure 1a indicates lower nonspecific binding with 500 nm particles, showing close to a 4-fold increase in binding of huA33 mAb-coated particles compared to controls.[16] The larger particles (1 μm) showed higher nonspecific binding, which could be due to the larger surface area of contact with the cell membrane. Also investigated were 300 nm particles, which exhibited similar binding to LIM1215 cells as the 1 μm particles (data not shown). This was attributed to the agglomeration of 300 nm particles to aggregates close to 1 μm in size, as evident under the fluorescence microscope. This suggests that the available surface area of contact with the cell may play a role in the nonspecific binding of the particles. The higher nonspecific binding observed with larger particles is also seen with the negative control cells, SW480, which do not express the A33 antigen (Figure 1b).

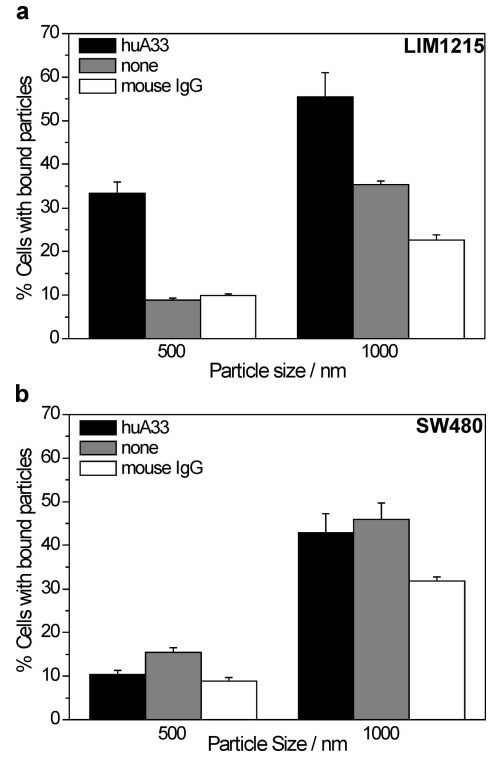

Figure 1. Effect of particle size on the selective binding of particles to cells. Binding of fluorescently labeled huA33 mAb-coated, noncoated, and mouse IgG-coated core–shell particles (500 nm and 1 μm) to (a) A33 antigen-expressing LIM1215 cells and (b) SW480 cells, which do not express the A33 antigen. The *y* axis shows the percentage of live cells with bound particles after 1 h of incubation at 4 °C, as analyzed by flow cytometry. Results represent the means of triplicate samples ± standard deviation.

The data suggest that, out of the three sizes investigated, the most favorable particle size for cell binding

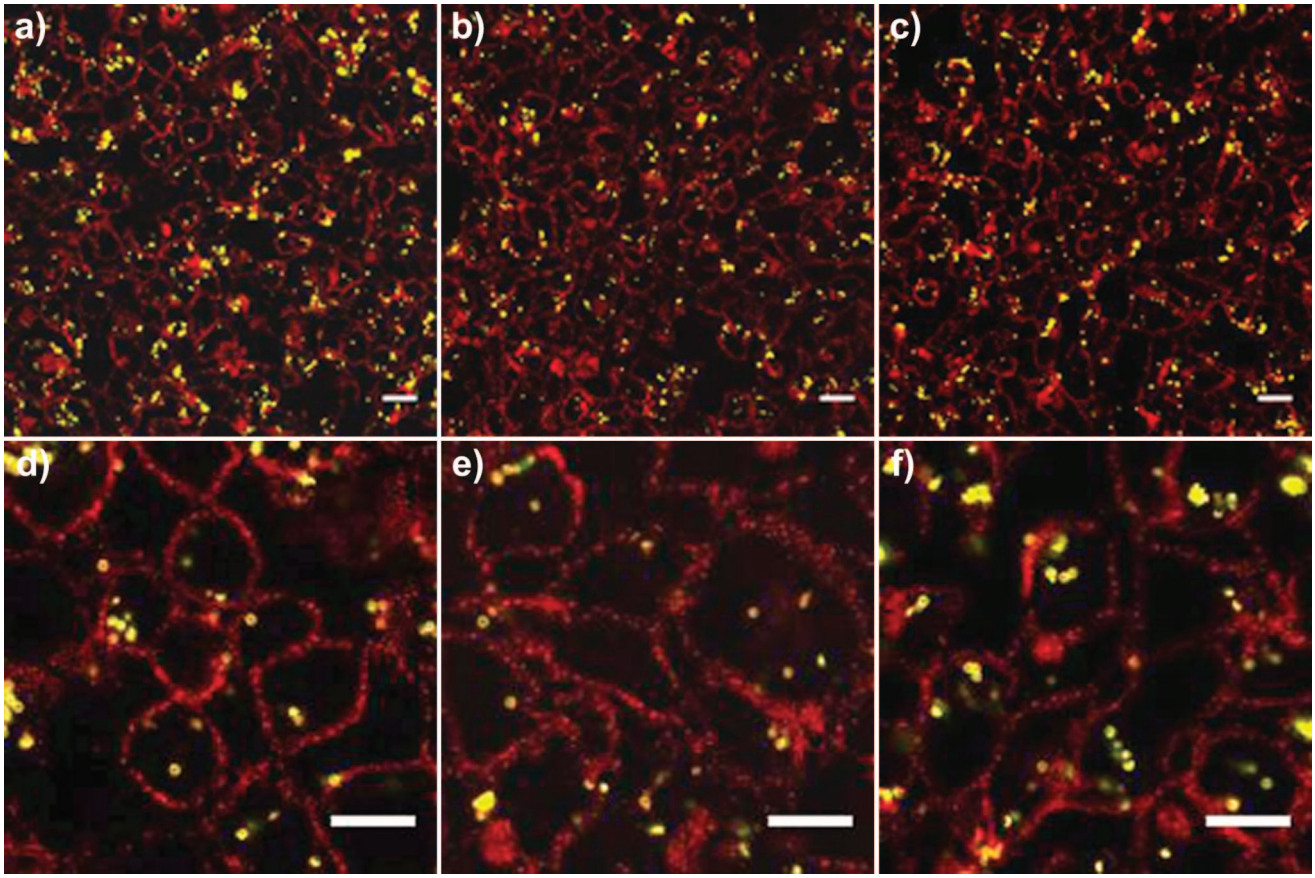

Figure 2. Binding and internalization of huA33 mAb-coated 1 μm core–shell particles by LIM1215 cells. Representative merged confocal laser scanning microscopy images of (a,d) huA33 mAb-coated, (b,e) noncoated, and (c,f) mouse IgG-coated, fluorescein-labeled particles (yellow) incubated with LIM1215 cells at 37 °C in a 5% CO_2 humidified atmosphere for 6 h to allow cellular uptake of particles. Cell membranes were counter-stained with a mouse mAb to the EGF receptor (mAb 528)[43] and detected with a TRITC-conjugated anti-mouse IgG secondary antibody (red). Scale bars, 10 μm.

is 500 nm. At this size, particles composed of PSS and poly(allylamine hydrochloride) (PAH) do not aggregate, and they exhibit low, nonspecific binding to cells. Core–shell particles and capsules of this size are within the size range that allows accessibility to tumor cells. It is well known that blood vessels supplying tumor cells are often "leaky", with most tumors exhibiting pores ranging from 380 to 780 nm.[41] The particles may therefore permeate through pores and be directed to the targeted cancer cells, where internalization of drug-loaded particles may take place. We have shown previously that binding of huA33 mAb-coated 500 nm particles to LIM1215 cells leads to their internalization.[16] Larger particles (1 μm) are also internalized by LIM1215 cells (see Figure 2), although internalization of these larger particles appears to be nonspecific, since high levels of internalization of mouse IgG-functionalized and nonfunctionalized particles were also observed. This is in accord with the binding data observed for 1 μm particles (Figure 1a). The data also suggest that initial binding to the cell, whether antigen-mediated or nonspecific, is a prerequisite for the subsequent internalization of a particle by the cell. It is therefore speculated that, although particle binding is specific, particle internalization occurs *via* a nonspecific endocytotic or phagocytotic mechanism. De Smedt and co-workers, in a study using LbL microcapsules composed of dextran sulfate and poly(arginine), have reported lipid raft-mediated uptake as a potential mechanism for LbL capsules internalization by VERO-1 cells.[42]

Effect of PSS–PEG on Cell Binding. The high, nonspecific binding observed for the 1 μm particles was investigated further using a polymer with nonfouling properties. A block copolymer of PSS and poly(ethylene glycol) (PSS–PEG) was deposited as the terminal layer of the core–shell particles prior to biofunctionalization with the antibody. PEG is a well-known nonfouling or protein-resistant polymer that is often used to coat surfaces to limit their interaction with biological interfaces.[14,44,45] PEG deposited on particles has been shown to decrease particle uptake by macrophages and increase the circulation of the particles.[13,45] As a block copolymer, PSS–PEG is expected to bind to positively charged surfaces due to its PSS component and exhibit a degree of nonfouling due to the PEG component. Figure 3a shows quartz crystal microgravimetry with dissipation capability (QCM-D) data confirming the binding of PSS–PEG to a PAH-terminated film on a planar sur-

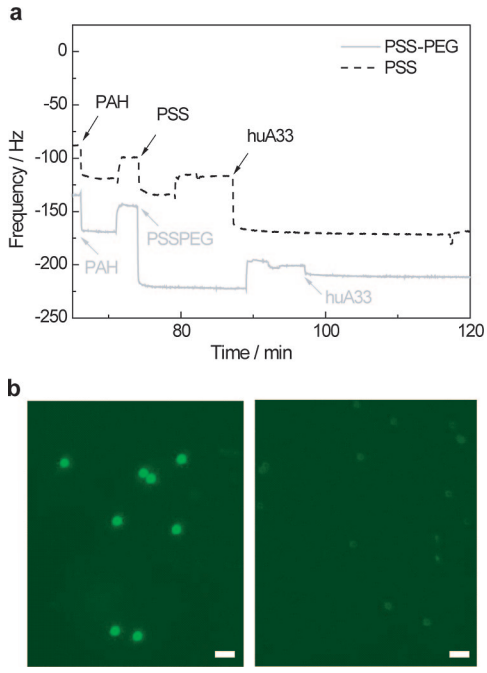

Figure 3. Characterization of huA33 mAb adsorption to PSS- and PSS–PEG-terminated surfaces. (a) HuA33 mAb binding to PSS [(PEI/PSS)(PAH/PSS)$_4$] and PSS–PEG [(PEI/PSS)(PAH/PSS)$_3$(PAH/PSS–PEG)] surfaces by QCM-D. (b) Fluorescence images of core–shell particles terminating with PSS (left) and PSS–PEG (right) after coating with fluorescein-labeled huA33 mAb and after three cycles of buffer washing. Scale bars, 2 μm.

face. The binding of PSS–PEG to PAH-terminated particles was characterized by microelectrophoresis, which showed a reversal of zeta-potential upon PSS–PEG binding to PAH (see Supporting Information). The characterization of binding of huA33 mAb to PSS–PEG compared to PSS by QCM-D is also shown in Figure 3a. Whereas the surface coverage of huA33 mAb on a PSS surface is approximately 10 mg m^{-2},[16] the surface coverage of huA33 mAb on a PSS–PEG surface is reduced to 0.9 mg m^{-2}, which is lower than the theoretically calculated surface coverage for a close-packed IgG monolayer (in the desired end-on orientation) of 3.7 mg m^{-2}.[46] Although a reduction in antibody adsorption to PSS–PEG compared to PSS was observed, as consistent with numerous studies on protein adsorption on PEG-modified surfaces, the huA33 mAb is still present and able to physically adsorb to the PSS–PEG surface (most likely *via* electrostatic bonding to the PSS component). This is confirmed by the adsorption of fluorescein-labeled huA33 mAb, with the resulting PSS–PEG particles showing an obvious decrease in green fluorescence compared with fluorescein-labeled huA33 mAb on PSS-terminated particles (Figure 3b). Figure 4 shows the binding of 1 μm huA33 mAb-coated, goat IgG-coated, and noncoated PSS- and PSS–PEG-terminated particles to LIM1215 cells. Particles 1 μm in size were investigated due to the high, nonspecific binding they exhibit, as shown above. A decrease in nonspecific binding (binding of control particles) is observed with PSS–PEG-terminated particles, while the binding of huA33 mAb-coated particles is slightly improved. In general, for 1 μm core–shell particles, close to a 5-fold increase in specific binding was observed with huA33 mAb-coated PSS–PEG particles (ratio of specific to nonspecific binding of 4.9 ± 0.4) compared with huA33 mAb-coated PSS particles (1.2 ± 0.2). This shows that PSS–PEG or polymers consisting partly of PEG can alleviate the nonspecific binding of particles to cells while maintaining a higher level of specific binding.

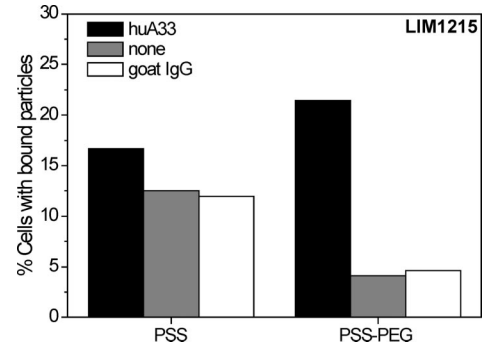

Figure 4. Comparison of the binding of PSS- and PSS–PEG-terminated particles to LIM1215 cells. Binding of 1 μm fluorescent PSS- and PSS–PEG-terminated core–shell particles coated with huA33 mAb-coated, goat IgG-coated, or noncoated to LIM1215 cells after 1 h of incubation at 4 °C, as analyzed by flow cytometry.

Effect of Particle Concentration or Dosage. The percentage of LIM1215 cells that bound 500 nm huA33 mAb-coated particles was typically in the range of 30–40% when incubated with a 0.004 wt % particle solution, or approximately 400 particles/cell.[16] With the aim of increasing specific binding, the effect of particle concentration on the degree of specific binding was investigated. The particle concentration of ~400 particles/cell, which represents coverage of a preset cell surface area of 100 μm^2, was normalized to 1. The binding of huA33 mAb-coated particles, compared with mouse IgG-coated particles, at the normalized ratios of 0.5 (~200 particles/cell), 1 (~400 particles/cell), 2 (~800 particles/cell), and 4 (~1600 particles/cell) is shown in Figure 5. The results show an increase in binding of 500 nm huA33 mAb-coated particles as particle number increases, with a dosage of 4 times the normalized particle concentration resulting in 50% of cells having particles bound on the surface. However, concurrent with this is the increase in the degree of nonspecific binding, as shown by the binding of mouse IgG-coated particles. These results show that there is scope in increasing the percentage of cells with bound particles by increasing the particle dosage, but the specificity of binding may be compromised. Nonspecific binding or passive delivery would be undesirable, as healthy cells would have a higher chance of taking up therapeutic-loaded particles. It would therefore be favorable to decrease nonspecific binding to improve the desired therapeutic ef-

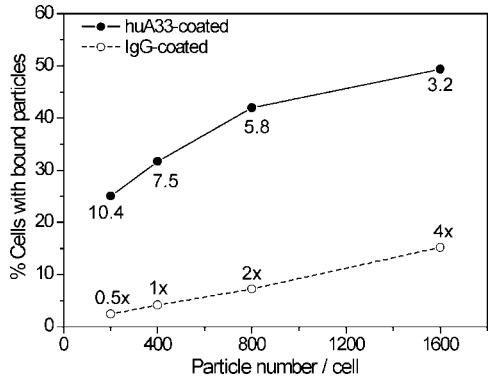

Figure 5. Effect of dosage on cellular binding. Flow cytometric analysis of the binding of increasing concentrations of 500 nm fluorescent PSS-terminated core–shell particles coated with huA33 mAb or mouse IgG to LIM1215 cells. The *y* axis shows the percentage of live cells with bound particles after 1 h of incubation at 4 °C. The values below the solid line represent the ratio of specific to nonspecific binding at each particle concentration. The values above the dotted line represent the normalized particle number, with 1× corresponding to ~400 particles/cell.

fects of the drug. A compromise must be sought to arrive at a particle ratio that increases the specific binding of huA33 mAb-coated particles yet maintains nonspecific binding to a low level. From the result in Figure 5, it appears that increasing the dosage to 2X or 800 particles/cell does not significantly increase the nonspecific binding of mouse IgG-coated particles to cells. In a separate study, the effect of the incubation time of the particles with the cells was explored. Increasing incubation time from 1 to 5 h did not lead to any further increase in cell binding (see Supporting Information).

Surface Effects. The influence of the outer surface prior to biofunctionalization[47] on the binding of the particles to cells was investigated. After the fourth PAH layer (layer 7), one of the following polymers was adsorbed: PSS, poly(acrylic acid) (PAA), poly(styrene sulfonate-*co*-maleic acid) (PSS–MA), poly(methacrylic acid) (PMA), or thiolated poly(methacrylic acid) (PMA_{SH}).[6,48,49] The physical adsorption of huA33 mAb to the various surfaces was characterized by QCM-D on a planar support and by microelectrophoresis for the particles. The properties of the 500 nm particles are shown in Table 1.

TABLE 1. Properties of 500 nm Multilayered (Core–Shell) Particles with Different Outer Surfaces and Binding Ratios for the LIM1215 Cells

polymer outer layer	zeta-potential (mV)[a]	zeta-potential (huA33 mAb-functionalized) (mV)[a]	huA33 mAb surface coverage (mg/m^2)[b]	binding ratio (huA33 mAb/control)[c]
PSS	−70 ± 1	−10 ± 3	8.3 ± 0.6	4.5 ± 1.4
PAH	13 ± 2	25 ± 1	3.2 ± 0.9	1.0 ± 0.2
PAA	−64 ± 1	−5 ± 5	10.9 ± 3.2	2.4 ± 0.8
PSS–MA	−68 ± 2	−7 ± 3	9.2 ± 0.3	3.3 ± 0.8
PMA	−69 ± 4	−6 ± 1	8.6 ± 1.0	1.7 ± 0.2
PMA_{SH}	−58 ± 8	−4 ± 1	10.7 ± 1.1	3.0 ± 0.9

[a]Dispersant: 20 mM HEPES, pH 7.2. [b]Determined using QCM-D. [c]Calculated from triplicate experiments. All results are means ± standard error.

The difference in the zeta-potentials, as measured by microelectrophoresis, of the noncoated and huA33 mAb-coated particles in 20 mM HEPES, pH 7.2, suggests that the antibody is tethered to the particle surface. This finding is confirmed by QCM-D studies, which were also used to estimate the relative surface coverage of huA33 mAb on the various surfaces (see Table 1).

The ratio of the binding of the 500 nm huA33 mAb-coated particles to the binding of the control particles (noncoated) is also shown in Table 1. In all cases except for the PAH outer surface, the presence of the huA33 mAb on the surface of the particles leads to an increase in binding by approximately 2–5-fold. Although the particles with the PSS outer layer showed the highest specific/nonspecific binding ratio of 4.5, the polyanions PSS–MA and PMA_{SH} also show promise as potential outer surfaces to which huA33 mAb can be deposited. Particles with a terminal PSS–MA layer have the added feature of carboxyl groups from the maleic acid component of PSS–MA, to which biomolecules can be covalently attached *via* amide linkages.[48] More importantly, capsules composed primarily of PMA_{SH}, which are stabilized solely through disulfide linkages, have the desirable characteristic of intracellular biodeconstructibility due to the reducing environment inside the cell.[6,12] The biofunctionalization of such capsules with an internalized protein like huA33 mAb would provide a mechanism with which PMA_{SH} capsules may be specifically internalized and subsequently deconstructed to release encapsulated materials. The thiol functionality of PMA_{SH} appears to contribute to improving the specificity of binding, as observed by comparing the binding ratios of PMA- and PMA_{SH}-terminated particles. While particles terminated with a polyanion prior to biofunctionalization showed some degree of specificity, particles terminating with PAH, a polycation, showed a high degree of nonspecific binding.[28] This was expected, as positively charged particles tend to bind nonspecifically to cells due to the overall negative charge on the cell surface, which is commonly exploited by commercially available polycationic cell transfection agents such as poly-L-lysine and cationic lipids.[50,51] The binding with PAH-coated particles has been found to be as high as 95% with LIM1215 cells, irrespective of the presence of a targeting ligand on the surface (data not shown). PAH-coated or polycation-coated particles and capsules would therefore be of use in applications where nonspecific delivery of material inside or in the local environment of cells is required, such as *in vitro* transfection.

Core–Shell Particles *vs* Capsules. For drug delivery purposes, capsules comprising a polymer shell and a liquid-filled interior will be more applicable in contrast to core–shell particles with a solid core. We compared the cellular binding of core–shell particles to the binding of capsules, both biofunctionalized with huA33 mAb or with mouse IgG or uncoated as controls, to

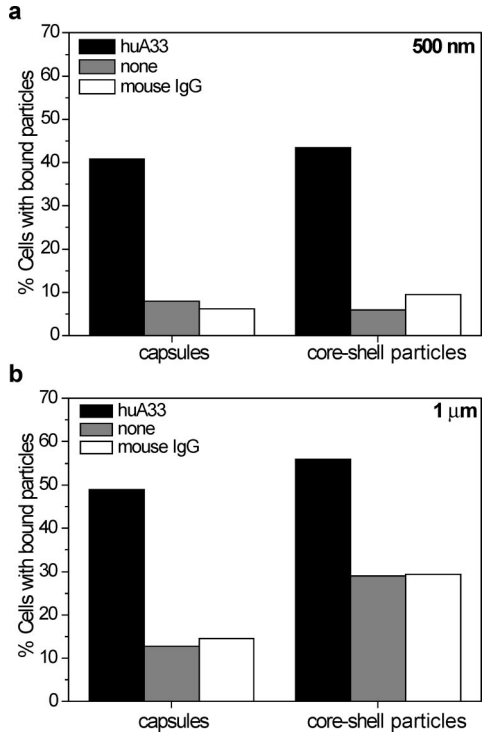

Figure 6. Comparison of the binding of core–shell particles *versus* capsules to LIM1215 cells. Flow cytometric data depicting the binding of (a) 500 nm and (b) 1 μm huA33 mAb-coated, noncoated, and mouse IgG-coated capsules compared with core–shell particles. The *y* axis shows the percentage of live cells with bound core–shell particles or capsules after 1 h of incubation at 4 °C.

LIM1215 cells. Figure 6 shows that the binding of 500 nm and 1 μm capsules is similar to that of core–shell particles. This was expected since the cores used in the core–shell particles are polystyrene spheres, which have a density similar to that of water. The main difference between the core–shell particles and capsules is, therefore, not in their masses but in their rigidity or flexibility. Compared to the more rigid structure of a core–shell particle, the capsule would have the flexibility to bend and contort, which may facilitate its way through gaps (*e.g.*, blood vessel pores or intercellular junctions) much smaller than its actual diameter.[52] Its ability to contort would hence reduce the effective surface area of contact with the cell interface. This may explain the lower nonspecific binding observed with the 1 μm capsules compared with the 1 μm core–shell particles, with the ratio of specific (huA33 mAb-coated) to nonspecific (noncoated) binding being 3.4 ± 0.3 and 1.8 ± 0.1 for 1 μm capsules and core–shell particles, respectively.

Our previous study showed that *core–shell particles* biofunctionalized with huA33 mAb lead to selective uptake by the A33 antigen-expressing colorectal cancer cell line, LIM1215. It was found that capsules are also internalized by LIM1215 cells (see Supporting Information) with a degree of specificity consistent with the binding data obtained from flow cytometry. The exact

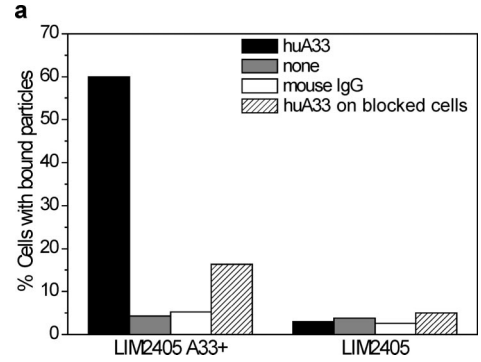

Figure 7. Binding of huA33-coated core–shell particles (diameter 500 nm) to other colorectal cancer cell lines: LIM2405 and LIM2405 A33+ (LIM2405 cells expressing recombinant A33 antigen). Representative data depicting the flow cytometric analysis of particle binding to live cells after 1 h of incubation with huA33-coated, noncoated, and mouse IgG-coated fluorescent particles at 4 °C. HuA33 mAb-coated particles were also added to preblocked cells (striped bars) to show specificity of binding to the A33 antigen.

mechanism of internalization is yet to be established, but our previous studies suggest that it is a consequence of A33 antigen-mediated binding.[16]

Binding to LIM2405 and LIM2405 A33+ Cells. The selective binding of huA33 mAb-coated particles was also tested on another set of colorectal cancer cell lines, LIM2405 and LIM2405 A33+, the latter being a clonal derivative of LIM2405 that expresses recombinant A33 antigen. Initial binding with fluorescein-labeled huA33 mAb confirmed the presence or lack of the A33 antigen on the surface of LIM2405 A33+ and LIM2405 cells, respectively (see Supporting Information). Flow cytometry data showing the binding of fluorescent core–shell particles coated with huA33 mAb, coated with mouse IgG, and noncoated to LIM2405 and LIM2405 A33+ cells are presented in Figure 7. The high binding (a 10-fold increase) of huA33 mAb-coated particles compared to the control particles shows their specific binding to LIM2405 A33+ cells. The specificity of the binding is indicated by the decrease in binding of the particles to LIM2405 A33+ cells that have been preblocked with free excess huA33 mAb. In addition, the nonspecific level of binding of huA33 mAb-coated particles to LIM2405 cells confirms that the binding of the particles is antigen-mediated. These results from two colorectal cancer-derived cell lines, which differ only in the expression of the A33 antigen, show that specific binding may also be achieved in other A33 antigen-expressing cells besides LIM1215 cells.

In conclusion, the influence of size, surface properties, cell line, and kinetic parameters such as dosage and incubation time on the binding specificity of huA33 mAb-coated LbL particles and capsules to colorectal cancer cells was investigated. The results showed various strategies in which the degree of specific binding can be improved. First, particles should be small enough to permeate through tumor blood vessels that have leaky pores up to about 800 nm in diameter and

can, at the same time, be prepared without significant aggregation. The particles with a negatively charged outer surface prior to biofunctionalization reduce nonspecific interaction with the negatively charged cells. Similarly, particles with an outer PSS-PEG surface also reduce nonspecific binding. The polyanions PSS, PSS–MA, and PMA_{SH} showed the most promising results, with the latter two allowing the possibility of covalent attachment of the targeting ligand. The results also show that the particles in the form of thin polymer hollow capsules will also exhibit specific binding similar to or better than that of core–shell particles and that simply increasing the dosage of the particles can improve the amount of binding to the cells. The huA33 mAb-functionalized particles showed significant enhancements in binding for both the LIM1215 and LIM2405 A33+ cells. The high and specific binding of huA33 mAb-coated particles and capsules to the A33 antigen, which is expressed by almost all primary colorectal cancer cells as well as colorectal cancer cell lines such as LIM1215 and LIM2405 A33+ cells, paves the way for further *in vitro* and *in vivo* studies of therapeutic drug loading and release from LbL capsules to colorectal cancer cells.

METHODS

Materials. Polystyrene particles (277 nm, 488 nm, and 0.98 μm in diameter) were purchased from MicroParticles GmbH, Germany. Poly(allylamine hydrochloride) (PAH; M_w 70 000 g mol^{-1}), poly(ethylenimine) (PEI; M_w 25 000 g mol^{-1}), poly(sodium 4-styrenesulfonate) (PSS; M_w 70 000 g mol^{-1}), poly(acrylic acid) (PAA; M_w 30 000 g mol^{-1}), and poly(4-styrenesulfonic acid-*co*-maleic acid (1:1 SS:MA, PSS–MA; M_w 20 000 g mol^{-1}) were purchased from Sigma-Aldrich and were used as received. Poly(methacrylic acid) (PMA; M_w 15 000 g mol^{-1}) was purchased from Polysciences, Inc. and was used as received. Thiolated PMA (PMA_{SH}) was a gift from Dr. A. Zelikin.[6] Poly(4-styrenesulfonate-*co*-ethylene glycol) (PSS–PEG; PSS M_w 52 000 g mol^{-1} (GPC); PEG M_w 26 000 g mol^{-1} (NMR)) was a gift from Prof. T. P. Davis, University of New South Wales, Australia.

The huA33 mAb and an antibody to the EGF receptor (mAb 528)[43] were produced in the Biological Production Facility at the Ludwig Institute for Cancer Research, Melbourne, Australia. The antibodies were dissolved in phosphate-buffered saline (PBS) containing 0.15 mM sodium azide (Sigma-Aldrich). Mouse IgG, goat IgG, and anti-human IgG (F_{ab} specific; Sigma-Aldrich) were dissolved in PBS. The washing or blocking buffer consisted of 10 mM ethylenediaminetetraacetic acid (EDTA), 1 wt % bovine serum albumin (BSA; Sigma-Aldrich), and 5% fetal calf serum (FCS; Thermotrace) in PBS, unless stated otherwise. 4-(2-Hydroxyethyl)-1-piperazineethanesulfonic acid (HEPES) was obtained from Sigma-Aldrich and was used at 20 mM, pH 7.2, unless stated otherwise.

Quartz crystal microgravimetry with dissipation (QCM-D) sensor electrodes (frequency = 5 mHz, AT-cut) were purchased from Q-Sense Corp. (Q-Sense AB, Göteberg, Sweden). The electrodes were cleaned three times with Piranha solution (concentrated sulfuric acid:hydrogen peroxide (30%), 7:3 (v/v)) and rinsed with copious amounts of Milli-Q water. (**Caution!** *Extreme care should be taken when handling Piranha solution as it is highly corrosive. It should only be prepared in small quantities.)* Tetrahydrofuran (THF) was from Lab-Scan Ltd., Ireland.

LIM1215, SW480, LIM2405, and LIM2405 A33+ (LIM2405 cells expressing recombinant A33 antigen) cell lines were all derived from human colorectal carcinoma. Cells were grown to subconfluency in RPMI 1640 medium supplemented with ADDS (10.8 μg mL^{-1} α-thioglycerol, 0.025 U mL^{-1} insulin, 1 μg mL^{-1} hydrocortisone, 60 μg mL^{-1} penicillin, and 12.6 μg mL^{-1} streptomycin) and 10% heat-inactivated FCS at 37 °C in a 5% CO_2 humidified atmosphere. The water used in all experiments was purified with a Millipore Rios/Synergy 2-stage purification system and had a resistivity greater than 18 MΩ cm.

Particle Size Effects. Core–shell particles of diameter approximately 300 nm, 500 nm, and 1 μm were prepared by the LbL deposition of PSS and PAH on 277 nm, 488 nm, and 0.98 μm polystyrene (PS) particles, respectively. Briefly, 500 μL of PAH was added to 200 μL of a 0.5 wt % PS particle suspension in water. Adsorption was carried out for 20 min, followed by centrifugation (10000*g* for 20 min, 12 min, and 6 min for 300 nm, 500 nm, and 1 μm particles, respectively). The supernatant was removed, and the particles were washed by redispersion in 500 μL of water, followed by centrifugation. The washing step was repeated a further two times before the particles were redispersed in 500 μL of water. An equal volume of PSS was then allowed to adsorb for 20 min and washed as described above. The process was repeated, with alternating layers of PAH or PAH-fluorescein and PSS, until eight layers of polyelectrolyte were deposited, with the outermost layer being PSS [$(PAH/PSS)_2$/(PAH-FITC/PSS)/(PAH/PSS)].

The PSS-terminated core–shell particles were coated with huA33 mAb (or mouse IgG) *via* physical adsorption. Each 1 mL of reaction mixture in HEPES buffer contained 0.14 mg mL^{-1} of huA33 mAb (or mouse IgG) and 50 μL of particles (or 100 μL for 1 μm particles). The mixture was incubated for 30 min at room temperature, with continuous mixing, followed by centrifugation at 4 °C. The supernatant was then replaced with 500 μL of HEPES. Washing by centrifugation and redispersion in HEPES were performed three times to remove unbound protein, and the washed particles were redispersed in 100 μL of HEPES and stored at 4 °C.

LIM1215 cells were used for the size-dependency study. For the particle binding investigation, the cells were washed with PBS before being detached from the surface with 10 mM EDTA in PBS at 37 °C in a 5% CO_2 humidified atmosphere for 10 min. Cells were aspirated gently to produce a single cell suspension, centrifuged at 400*g* for 3 min, and resuspended in washing buffer. For all remaining procedures, cells were kept on ice to prevent internalization of antigen-bound particles. HuA33 mAb-coated, mouse IgG-coated, and noncoated fluorescein-labeled particles were added to 1 mL of 10^6 cells (1 μm particles, 50 μL of 0.2 wt %; 500 nm particles, 40 μL of 0.1 wt %; 300 nm particles, 20 μL of 0.1 wt %). Incubation was carried out for 1 h on ice with occasional gentle shaking. Cells with bound particles were then pelleted by centrifugation at 340*g* for 4 min and resuspended in 0.5 mL of washing buffer containing 5 μg mL^{-1} propidium iodide (PI, Sigma-Aldrich) for flow cytometry using a Becton Dickinson FACScalibur. Forty thousand events were counted. Flow cytometry data analysis was performed with Summit v3.1 (Cytomation, Inc., Fort Collins, CO), taking into account live cells only (PI negative). The background was set at 1% during flow cytometry data analysis unless otherwise stated.

For the particle internalization investigation, LIM1215 cells were seeded onto 25 mm diameter glass cover slips in six-well tissue culture plates at a density of 10^6 cells/well and left to grow overnight. Cells adhered to cover slips were washed three times in serum-free RPMI 1640 medium supplemented with ADDS and returned to 37 °C in a 5% CO_2 humidified atmosphere for 30 min prior to incubation with particles. HuA33 mAb-coated, mouse IgG-coated, and noncoated, fluorescein-labeled 1 μm particles in RPMI 1640 medium supplemented with ADDS were added to LIM1215 cells (100 particles/cell) and incubated at 37 °C in a 5% CO_2 humidified atmosphere for 6 h to allow cellular uptake of particles. Following incubation, cells were washed three times in ice-cold RPMI 1640 medium supplemented with ADDS and 1% BSA to remove unbound particles. Cell membranes were counterstained at 4 °C with a monoclonal antibody to the EGF re-

ceptor (mAb 528) and detected with TRITC-conjugated anti-mouse IgG secondary antibody. Cells were fixed with 4% paraformaldehyde. Confocal microscopy images were obtained using a Leica laser-scanning confocal unit (TCS SP2; Leica, Germany).

Dosage Effects. HuA33 mAb- and mouse IgG-coated fluorescein-labeled core–shell particles (~500 nm) were incubated with 10^6 cells at various final concentrations: 0.002 (0.5×), 0.004 (1×), 0.008 (2×), and 0.016 wt % (4×) particles/cell. A final concentration of 0.004 wt %, or ~400 particles/cell, which represents coverage of a preset cell surface area of 100 μm^2, was denoted as 1×. Excess (unbound) particles were removed by centrifugation prior to analysis by flow cytometry, as described above.

Effect of PEG on Specific Binding. Core–shell particles consisting of eight layers and terminating with PSS–PEG were prepared [$(PAH/PSS)_2$/(PAH-FITC/PSS)/(PAH/PSS–PEG)] using 0.98 μm PS cores. PSS–PEG was deposited at 1 mg mL^{-1} containing 0.5 M NaCl. After three washing cycles in water, the particles were coated with huA33 mAb and goat IgG, as described above. LIM1215 cells were incubated with coated particles (100 particles/cell), and particle binding was analyzed by flow cytometry, as described above. Characterization of huA33 mAb adsorption to PSS–PEG was carried out using fluorescence microscopy and QCM-D (see below).

Surface Chemistry. Core–shell particles (~500 nm diameter) consisting of seven layers of PAH and PSS on a PS core were prepared [$(PAH/PSS)_2$/(PAH-FITC/PSS)/PAH]. The surface of the particles was varied by adsorbing various polyanions (PSS, PSS–MA, PMA, PMA_{SH}, and PAA) to PAH-terminated particles. All polyanions were deposited at 1 mg mL^{-1} containing 0.5 M NaCl. After three washing cycles in water, the various particles (including PAH-terminated particles) were coated with huA33 mAb and mouse IgG, as described above. Characterization of huA33 mAb adsorption to the various surfaces was carried out by microelectrophoresis on the particles and QCM-D on planar surfaces. Particle incubation with LIM1215 cells and subsequent analysis by flow cytometry were carried out as described earlier.

Influence of Core–Shell Particles *vs* Capsules on Cell Binding. Capsules of ~500 nm and 1 μm diameter were prepared by dissolving the PS core with THF. To dissolve the core, THF (2 mL) was added to the core–shell particles (pelleted) and incubated overnight with continuous mixing. The partially dissolved particles were centrifuged (1000*g*, 15 and 20 min for 1 μm and 500 nm capsules, respectively), redispersed in 2 mL of THF, and incubated further (overnight). The capsule dispersion was then centrifuged, washed three times with water (500 μL), and resuspended in 500 μL of water. Biofunctionalization of the capsules with huA33 mAb or mouse IgG and subsequent cell binding analysis by flow cytometry were performed as described for the core–shell particles.

Zeta-Potential. Microelectrophoresis (ZetaSizer 2000, Malvern Instruments) was employed to measure the zeta-potential of the particles before and after huA33 mAb adsorption. The average of five successive measurements in 20 mM HEPES, pH 7.2, was taken (±standard deviation).

Fluorescence Microscopy. To confirm the binding of huA33 mAb to the particles, fluorescein-labeled huA33 mAb (FITC-huA33 mAb) was used. Briefly, 3 μL of 4 mg mL^{-1} FITC in dimethylsulfoxide (DMSO) was added to 1 mL of 1 mg mL^{-1} huA33 mAb in 0.05 M sodium bicarbonate buffer, pH 9.3. The mixture was incubated overnight at 4 °C and dialyzed against PBS, pH 7.2, over 72 h (with buffer replacement every 24 h) at 4 °C. FITC-huA33 mAb was adsorbed onto particles as described earlier. Fluorescence microscopy images of the particles were obtained with an Olympus 1X71 inverted microscope using a blue excitation filter.

QCM-D Investigation of HuA33 mAb Binding to Various Surfaces. The formation of multilayer thin films consisting of PAH and PSS and terminating with various polyanions, and the subsequent biofunctionalization of the various films by physical adsorption of huA33 mAb, were followed by QCM-D. PEI (1 mg mL^{-1}, 0.5 M NaCl) was deposited on the electrode as the first layer (15 min incubation). Sequential deposition of PSS (1 mg mL^{-1}, 0.5 M NaCl) and PAH (1 mg mL^{-1}, 0.5 M NaCl) (15 min adsorption, 5 min washing, or until no further change in frequency was recorded) was repeated until eight layers of PSS and PAH were adsorbed. PSS, PSS–PEG, PSS–MA, PMA, PMA_{SH}, or PAA was then deposited as the outer layer. The film was rinsed with HEPES buffer for 10 min before the introduction of huA33 mAb (200 μg mL^{-1}) in the measurement chamber. Physical adsorption of the antibody was measured for 30 min, after which the surface was rinsed with HEPES buffer (5 min) to remove unbound antibody. Following blocking with washing buffer containing BSA and FCS (30 min adsorption and then a 5 min rinse with HEPES), subsequent interaction with anti-human IgG (F_{ab} specific) was investigated by introducing the antibody (200 μg mL^{-1}, 3 h adsorption, 5 min rinse) to the blocked huA33 mAb-coated film. QCM-D data were collected from the fifth overtone of the resonant frequency. The sample chamber was maintained at a constant temperature of 23.5 ± 0.1 °C for all measurements.

Binding to LIM2405 and LIM2405 A33+ Cells. The binding of huA33 mAb-coated particles (500 nm) to A33 antigen negative LIM2405 cells and LIM2405 into which human A33 antigen cDNA had been installed (LIM2405 A33+) was investigated to confirm binding specificity. LIM2405 and LIM2405 A33+ cells were grown to subconfluency at 37 °C in a 5% CO_2 humidified atmosphere. Cells were washed with prewarmed PBS before being detached from the surface with 2 mM EDTA in PBS at 37 °C in a 5% CO_2 humidified atmosphere for 10 min. Cells were aspirated gently to produce a single cell suspension, centrifuged at 400*g* for 3 min, and resuspended in washing buffer. For all remaining procedures, cells were kept on ice to prevent internalization of antigen-bound particles. Core–shell particles (500 nm) were incubated with the cells, and the binding was analyzed by flow cytometry as described earlier. As a further test for specificity, cells were preblocked by incubating with huA33 mAb to a final concentration of 70 μg mL^{-1} for 30 min on ice before addition of huA33 mAb-coated particles, as described above. A33 antigen expression was determined by incubation of 10^6 cells with 20 μg mL^{-1} fluorescein-labeled huA33 mAb. Background was set at 0.01% during flow cytometry data analysis.

Acknowledgment. This work was supported by the Australian Research Council under the Federation Fellowship (F.C.) and Discovery Project (F.C.) schemes, the Victorian State Government under the STI Initiative, and the National Health and Medical Research Council (NHMRC), Project Grant 433613 (J.K.H., F.C., E.C.N.). E.T.-C. was supported by an NHMRC Dora Lush Postgraduate Research Scholarship. E.C.N. and A.M.S. were supported, in part, by NHMRC Project Grants 191500, 164809, and 164814, and Program Grant 280912. The Particulate Fluids Processing Centre is gratefully acknowledged for infrastructural support. Amon Carson is acknowledged for his assistance with capsule preparation.

Supporting Information Available: Binding of PSS–PEG to PAH-terminated particles; effect of incubation time on particle binding to cells; internalization of 500 nm *capsules* by LIM1215 cells; and flow cytometric analysis of A33 antigen expression of LIM2405 and LIM2405 A33+. This material is available free of charge *via* the Internet at http://pubs.acs.org.

REFERENCES AND NOTES

1. Johnston, A. P. R.; Cortez, C.; Angelatos, A. S.; Caruso, F. Layer-by-Layer Engineered Capsules and Their Applications. *Curr. Opin. Colloid Interface Sci.* **2006**, *11*, 203–209.
2. Peyratout, C. S.; Dahne, L. Tailor-Made Polyelectrolyte Microcapsules: From Multilayers to Smart Containers. *Angew. Chem., Int. Ed.* **2004**, *43*, 3762–3783.
3. Angelatos, A. S.; Katagiri, K.; Caruso, F. Bioinspired Colloidal Systems via Layer-by-Layer Assembly. *Soft Matter* **2006**, *2*, 18–23.
4. Donath, E.; Sukhorukov, G. B.; Caruso, F.; Davis, S. A.; Moehwald, H. Novel Hollow Polymer Shells by Colloid-Templated Assembly of Polyelectrolytes. *Angew. Chem., Int. Ed.* **1998**, *37*, 2202–2205.
5. Caruso, F.; Caruso, R. A.; Moehwald, H. Nanoengineering of Inorganic and Hybrid Hollow Spheres by Colloidal Templating. *Science* **1998**, *282*, 1111–1114.

6. Zelikin, A. N.; Quinn, J. F.; Caruso, F. Disulfide Cross-Linked Polymer Capsules: En Route to Biodeconstructible Systems. *Biomacromolecules* **2006**, *7*, 27–30.
7. Such, G. K.; Tjipto, E.; Postma, A.; Johnston, A. P.; Caruso, F. Ultrathin, Responsive Polymer Click Capsules. *Nano Lett.* **2007**, *7*, 1706–1710.
8. Wang, Y. J.; Caruso, F. Enzyme Encapsulation in Nanoporous Silica Spheres. *Chem. Commun.* **2004**, *13*, 1528–1529.
9. Caruso, F.; Trau, D.; Mohwald, H.; Renneberg, R. Enzyme Encapsulation in Layer-by-Layer Engineered Polymer Multilayer Capsules. *Langmuir* **2000**, *16*, 1485–1488.
10. Balabushevich, N. G.; Tiourina, O. P.; Volodkin, D. V.; Larionova, N. I.; Sukhorukov, G. B. Loading the Multilayer Dextran Sulfate/Protamine Microsized Capsules with Peroxidase. *Biomacromolecules* **2003**, *4*, 1191–1197.
11. Khopade, A. J.; Caruso, F. Stepwise Self-assembled Poly(amidoamine) Dendrimer and Poly(styrenesulfonate) Microcapsules as Sustained Delivery Vehicles. *Biomacromolecules* **2002**, *3*, 1154–1162.
12. Zelikin, A. N.; Li, Q.; Caruso, F. Degradable Polyelectrolyte Capsules Filled with Oligonucleotide Sequences. *Angew. Chem., Int. Ed.* **2006**, *45*, 7743–7745.
13. Khopade, A. J.; Caruso, F. Surface-Modification of Polyelectrolyte Multilayer-Coated Particles for Biological Applications. *Langmuir* **2003**, *19*, 6219–6225.
14. Heuberger, R.; Sukhorukov, G.; Voros, J.; Textor, M.; Moehwald, H. Biofunctional Polyelectrolyte Multilayers and Microcapsules: Control of Non-specific and Bio-specific Protein Adsorption. *Adv. Funct. Mater.* **2005**, *15*, 357–366.
15. Fischlechner, M.; Zschornig, O.; Hofmann, J.; Donath, E. Engineering Virus Functionalities on Colloidal Polyelectrolyte Lipid Composites. *Angew. Chem., Int. Ed.* **2005**, *44*, 2892–2895.
16. Cortez, C.; Tomaskovic-Crook, E.; Johnston, A. P. R.; Radt, B.; Cody, S. H.; Scott, A. M.; Nice, E. C.; Heath, J. K.; Caruso, F. Targeting and Uptake of Multilayered Particles to Colorectal Cancer Cells. *Adv. Mater.* **2006**, *18*, 1998–2003.
17. Torchilin, V. P. Drug Targeting. *Eur. J. Pharm. Sci.* **2000**, *11*, S81–91.
18. Win, K. Y.; Feng, S. S. Effects of Particle Size and Surface Coating on Cellular Uptake of Polymeric Nanoparticles for Oral Delivery of Anticancer Drugs. *Biomaterials* **2005**, *26*, 2713–2722.
19. Pang, S. W.; Park, H. Y.; Jang, Y. S.; Kim, W. S.; Kim, J. H. Effects of Charge Density and Particle Size of Poly(styrene/(dimethylamino)ethyl methacrylate) Nanoparticle for Gene Delivery in 293 cells. *Colloids Surf. B: Biointerfaces* **2002**, *26*, 213–222.
20. Foged, C.; Brodin, B.; Frokjaer, S.; Sundblad, A. Particle Size and Surface Charge Affect Particle Uptake by Human Dendritic Cells in an In Vitro Model. *Int. J. Pharm.* **2005**, *298*, 315–322.
21. Pinaud, F.; King, D.; Moore, H. P.; Weiss, S. Bioactivation and Cell Targeting of Semiconductor CdSe/ZnS Nanocrystals with Phytochelatin-Related Peptides. *J. Am. Chem. Soc.* **2004**, *126*, 6115–6123.
22. Tkachenko, A. G.; Xie, H.; Coleman, D.; Glomm, W.; Ryan, J.; Anderson, M. F.; Franzen, S.; Feldheim, D. L. Multifunctional Gold Nanoparticle-Peptide Complexes for Nuclear Targeting. *J. Am. Chem. Soc.* **2003**, *125*, 4700–4701.
23. Zebli, B.; Susha, A. S.; Sukhorukov, G. B.; Rogach, A. L.; Parak, W. J. Magnetic Targeting and Cellular Uptake of Polymer Microcapsules Simultaneously Functionalized with Magnetic and Luminescent Nanocrystals. *Langmuir* **2005**, *21*, 4262–4265.
24. Turan, K.; Nagata, K. Chitosan-DNA Nanoparticles: The Effect of Cell Type and Hydrolysis of Chitosan on In Vitro DNA Transfection. *Pharm. Dev. Technol.* **2006**, *11*, 503–512.
25. Wartlick, H.; Michaelis, K.; Balthasar, S.; Strebhardt, K.; Kreuter, J.; Langer, K. Highly Specific HER2-Mediated Cellular Uptake of Antibody-Modified Nanoparticles in Tumour Cells. *J. Drug Targeting.* **2004**, *12*, 461–471.
26. Sherbet, G. V.; Lakshimi, M. S.; Rao, K. V. Characterisation of Ionogenic Groups and Estimation of the Net Negative Electric Charge on the Surface of Cells Using Natural pH Gradients. *Exp. Cell Res.* **1972**, *70*, 113–123.
27. Ahmed, K.; Nakagawa, T.; Nakano, Y.; Martinez, G.; Ichinose, A.; Zheng, C. H.; Akaki, M.; Aikawa, M.; Nagatake, T. Attachment of Moraxella Catarrhalis Occurs to the Positively Charged Domains of Pharyngeal Epithelial Cells. *Microb. Pathogenesis* **2000**, *28*, 203–209.
28. Reibetanz, U.; Claus, C.; Typlt, E.; Hofmann, J.; Donath, E. Defoliation and Plasmid Delivery with Layer-by-Layer Coated Colloids. *Macromol. Biosci.* **2006**, *6*, 153–160.
29. De, S.; Miller, D. W.; Robinson, D. H. Effect of Particle Size of Nanospheres and Microspheres on the Cellular-Association and Cytotoxicity of Paclitaxel in 4T1 Cells. *Pharm. Res.* **2005**, *22*, 766–775.
30. Welt, S.; Divgi, C. R.; Real, F. X.; Yeh, S. D.; Garin-Chesa, P.; Finstad, C. L.; Sakamoto, J.; Cohen, A.; Sigurdson, E. R.; Kemeny, N.; et al. Quantitative Analysis of Antibody Localization in Human Metastatic Colon Cancer: A Phase I Study of Monoclonal Antibody A33. *J. Clin. Oncol.* **1990**, *8*, 1894–1906.
31. Heath, J. K.; White, S. J.; Johnstone, C. N.; Catimel, B.; Simpson, R. J.; Moritz, R. L.; Tu, G. F.; Ji, H.; Whitehead, R. H.; Groenen, L. C.; et al. The Human A33 Antigen is a Transmembrane Glycoprotein and a Novel Member of the Immunoglobulin Superfamily. *Proc. Natl. Acad. Sci. U.S.A.* **1997**, *94*, 469–474.
32. Daghighian, F.; Barendswaard, E.; Welt, S.; Humm, J.; Scott, A.; Willingham, M. C.; McGuffie, E.; Old, L. J.; Larson, S. M. Enhancement of Radiation Dose to the Nucleus by Vesicular Internalization of Iodine-125-Labeled A33 Monoclonal Antibody. *J. Nucl. Med.* **1996**, *37*, 1052–1057.
33. Welt, S.; Ritter, G.; Williams, C., Jr.; Cohen, L. S.; John, M.; Jungbluth, A.; Richards, E. A.; Old, L. J.; Kemeny, N. E. Phase I Study of Anticolon Cancer Humanized Antibody A33. *Clin. Cancer Res.* **2003**, *9*, 1338–1346.
34. Scott, A. M.; Lee, F. T.; Jones, R.; Hopkins, W.; MacGregor, D.; Cebon, J. S.; Hannah, A.; Chong, G.; U, P.; Papenfuss, A. A Phase I Trial of Humanized Monoclonal Antibody A33 in Patients with Colorectal Carcinoma: Biodistribution, Pharmacokinetics, and Quantitative Tumor Uptake. *Clin. Cancer Res.* **2005**, *11*, 4810–4817.
35. Chong, G.; Lee, F. T.; Hopkins, W.; Tebbutt, N.; Cebon, J. S.; Mountain, A. J.; Chappell, B.; Papenfuss, A.; Schleyer, P.; U, P. Phase I Trial of 131I-HuA33 in Patients with Advanced Colorectal Carcinoma. *Clin. Cancer Res.* **2005**, *11*, 4818–4826.
36. Caruso, F.; Niikura, K.; Furlong, D. N.; Okahata, Y. 2. Assembly of Alternating Polyelectrolyte and Protein Multilayer Films for Immunosensing. *Langmuir* **1997**, *13*, 3427–3433.
37. Jessel, N.; Oulad-Abdelghani, M.; Meyer, F.; Lavalle, P.; Haikel, Y.; Schaaf, P.; Voegel, J. C. Multiple and Time-Scheduled In Situ DNA Delivery Mediated by Beta-Cyclodextrin Embedded in a Polyelectrolyte Multilayer. *Proc. Natl. Acad. Sci. U.S.A.* **2006**, *103*, 8618–8621.
38. Benkirane-Jessel, N.; Lavalle, P.; Meyer, F.; Audouin, F.; Frisch, B.; Schaaf, P.; Ogier, J.; Decher, G.; Voegel, J. C. Control of Monocyte Morphology on and Response to Model Surfaces for Implants Equipped with Anti-Inflammatory Agents. *Adv. Mater.* **2004**, *16*, 1507–1511.
39. Dierich, A.; Le Guen, E.; Messaddeq, N.; Stoltz, J.-F.; Netter, P.; Schaaf, P.; Voegel, J.-C.; Benkirane-Jessel, N. Bone Formation Mediated by Synergy-Acting Growth Factors Embedded in a Polyelectrolyte Multilayer Film. *Adv. Mater.* **2007**, *19*, 693–697.
40. Leguen, E.; Chassepot, A.; Decher, G.; Schaaf, P.; Voegel, J.-C.; Jessel, N. Bioactive Coatings Based on Polyelectrolyte Multilayer Architectures Functionalized by Embedded Proteins, Peptides or Drugs. *Biomol. Eng.* **2007**, *24*, 33–41.
41. Hobbs, S. K.; Monsky, W. L.; Yuan, F.; Roberts, W. G.; Griffith, L.; Torchilin, V. P.; Jain, R. K. Regulation of Transport Pathways in Tumor Vessels: Role of Tumor Type and

Microenvironment. *Proc. Natl. Acad. Sci. U.S.A.* **1998**, *95*, 4607–4612.
42. De Geest, B. G.; Vandenbroucke, R. E.; Guenther, A. M.; Sukhorukov, G. B.; Hennick, W. E.; Sanders, N. N.; Demeester, J.; De Smedt, S. C. Intracellularly Degradable Polyelectrolyte Microcapsules. *Adv. Mater.* **2006**, *18*, 1005–1009.
43. Gill, G. N.; Kawamoto, T.; Cochet, C.; Le, A.; Sato, J. D.; Masui, H.; McLeod, C.; Mendelsohn, J. Monoclonal Anti-Epidermal Growth Factor Receptor Antibodies which are Inhibitors of Epidermal Growth Factor Binding and Antagonists of Epidermal Growth Factor Binding and Antagonists of Epidermal Growth Factor-Stimulated Tyrosine Protein Kinase Activity. *J. Biol. Chem.* **1984**, *259*, 7755–7760.
44. Jenney, C. R.; Anderson, J. M. Effects of Surface-Coupled Polyethylene Oxide on Human Macrophage Adhesion and Foreign Body Giant Cell Formation In Vitro. *J. Biomed. Mater. Res.* **1999**, *44*, 206–216.
45. Blume, G.; Cevc, G. Liposomes for the Sustained Drug Release In Vivo. *Biochim. Biophys. Acta* **1990**, *1029*, 91–97.
46. Buijs, J.; Lichtenbelt, J. W. T.; Norde, W.; Lyklema, J. Adsorption of Monoclonal IgGs and Their F(Ab')(2) Fragments onto Polymeric Surfaces. *Colloids Surf. B: Biointerfaces* **1995**, *5*, 11–23.
47. Ladam, G.; Schaaf, P.; Cuisinier, F. J. G.; Decher, G.; Voegel, J.-C. Protein Adsorption onto Auto-Assembled Polyelectrolyte Films. *Langmuir* **2001**, *17*, 878–882.
48. Tjipto, E.; Quinn, J. F.; Caruso, F. Assembly of Multilayer Films from Polyelectrolytes Containing Weak and Strong Acid Moieties. *Langmuir* **2005**, *21*, 8785–8792.
49. Yap, H. P.; Quinn, J. F.; Ng, S. M.; Cho, J. H.; Caruso, F. Colloid Surface Engineering via Deposition of Multilayered Thin Films from Polyelectrolyte Blend Solutions. *Langmuir* **2005**, *21*, 4328–4333.
50. Godbey, W. T.; Mikos, A. G. Recent Progress in Gene Delivery Using Non-Viral Transfer Complexes. *J. Controlled Release* **2001**, *72*, 115–125.
51. Holtorf, H. L.; Mikos, A. G. Cationic and Non-Condensing Polymer-Based Gene Delivery. In *Pharmaceutical Perspectives of Nucleic Acid-Based Therapeutics*; Kim, S. W., Mahato, R. I., Eds.; Taylor & Francis: New York, 2002; pp 367–387.
52. Prevot, M.; Cordeiro, A. L.; Sukhorukov, G. B.; Lvov, Y.; Besser, R. S.; Moehwald, H. Design of a Microfluidic System to Investigate the Mechanical Properties of Layer-by-Layer Fabricated Capsules. *Macromol. Mater. Eng.* **2003**, *288*, 915–919.